Study of the Corrosion Resistance of Ni/CeO_2 Composite Coatings Electrodeposited on Carbon Steel in Hydrochloric Acid

A. Samide* **and B. Tutunaru**
University of Craiova, Faculty of Chemistry,
Calea Bucuresti 107i, Craiova, Romania

Original scientific paper
Received: July 20, 2010
Accepted: May 4, 2011

The phase formation of Ni-Ce composites onto a carbon steel electrode was investigated using electrochemical deposition. The anticorrosive properties of composite coating in 0.1 mol L^{-1} HCl solution were studied by Tafel polarization and electrochemical impedance spectroscopy (EIS). Incorporation of CeO_2 particles into the Ni matrices was found to improve corrosion resistance of pure Ni coatings. The values of protection efficiency obtained from Tafel polarization and EIS measurements are in good agreement, reaching a maximum value of 57 %, at 0.1 g L^{-1} CeO_2 containing electro-deposition bath. The surface morphologies and compositions of coatings were studied using scanning electron microscopy with Energy Dispersive X-ray Spectroscopy (SEM/EDS). In case of electro-depositions from solution containing CeO_2 (Fig. 3c) the layer uniformity is more apparent and the feature of a metalic nucleation, forming a matrix in which are embedded certain oxide particle is relatively nuanced.

Key words:
Carbon steel, electro-deposition, Ni/CeO_2 composite, corrosion resistance

Introduction

Composite coatings obtained by co-deposition of different dispersed phases have been given special attention in recent years.

A considerable number of literature studies cite the enhanced properties resulting from suspending an insoluble material in a conventional plating electrolyte and capturing them in the growing metallic film.

Ni-based composites generally designed for high temperature applications, possess some characteristics such as good thermal stability, chemical inertness, yield and tensile strength, and wear resistance compared to pure nickel. Composites (SiC,[1–5] Al_2O_3,[6–8] TiO_2,[9,10] ZrO_2,[11–13] La_2O_3,[14] SiO_2-Al_2O_3,[15] CeO_2-Al_2O_3/Y_2O_3,[16,17] Al_2O_3/CeO_2-Ce_2O_3,[18–22] polymers (polyethylene,[23] polytetrafluorethylene[24]), metals and other materials (hydroxyapatite,[25] diamond,[26] fullerene,[27] carbon fibers[28]) have been co-electrodeposited with nickel in order to improve their properties. The main parameters that influence the properties of the composites are electrolyte composition, pH, temperature, cathodic current density, stirring rate of the solution and particle concentration and size.

The present work aims to study the corrosion resistance of Ni/CeO_2 composite coatings electro-deposited on carbon steel, in 0.1 mol L^{-1} hydrochloric acid.

*Corresponding author: E-mail address: samide_adriana@yahoo.com, Phone/Fax: +040251-597048

Materials and methods

Coatings electro-deposition

Electrochemical measurements for Ni and Ni-CeO_2 electrodeposition were performed with the Keithley 2420 3A SourceMeter potentiostat/galvanostat. Experimental data recording was carried out in a standard electrochemical cell with three electrodes. The Ag/AgCl, KCl (saturated) was used as the reference electrode to which all potentials are quoted. The working electrode was made from carbon steel, the auxiliary electrode was made from nickel foils with 1.0 cm^2 geometric area. The Ni films were deposited onto carbon steel (with surface area of 1.0 cm^2) by potentiodynamic polarisation, with a scan rate of 50 mV/10 sec. The carbon steel (type C38) used had the following composition (mass/%): C = 0.1 %; Si = 0.035 %; Mn = 0.4 %; Cr = 0.3 %; Ni = 0.3 %, with the balance in Fe. The polished carbon steel substrate was degreased with acetone, and washed with distilled water. The electrolyte bath for Ni deposition comprised of 150 g L^{-1} $NiSO_4 \cdot 6H_2O$, 30 g L^{-1} H_3BO_3 aqueous solution (pH = 2 ± 0.05) and the working temperature was of 20 ± 2 °C. To ensure a uniform dispersion of micro-particles, the electrolyte was stirred for 2 h before the deposition. The pH of the electrolytic bath was measured using digital pH-meter (HANNA instruments).

In the electrolyte bath for Ni-ceria electrodeposition, the concentration of added CeO_2 was of 0.1 and 0.3 g L^{-1}. The stirring rate was kept constant at 300 rpm.

Corrosion tests

Electrochemical measurements were conducted using an electrochemical system, VoltaLab 40, with a personal computer and VoltaMaster 4 software. A standard corrosion cell was used. A platinum plate (1 cm^2) and Ag/AgCl electrode were used as auxiliary and reference electrodes, respectively. The immersion time of the plates in the respective media was 1 minute in open circuit, at room temperature. Potentiodynamic polarization curves were obtained with the scan rate of 10 mV s^{-1}.

Electrochemical impedance spectroscopy (EIS) was measured in a frequency range from 100 kHz to 10 mHz by a parturition signal of 10 mV amplitude peak to peak at room temperature, after the immersion time of 1 minute in open circuit. Potentiodynamic polarization and EIS data were analyzed by means of *Excel* and *Zview*, respectively.

Surfaces characterization

The morphologies of the coatings and the elemental components were inspected by SEM and EDS on Vega Tescan scanning electron microscope.

Results and discussion

Powder morphology

The micro-sized nature of the powder was evidenced by SEM. The typical powder morphology is shown in Fig. 1.

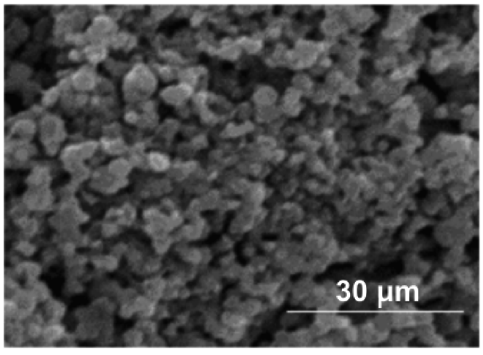

F i g . 1 – *SEM image of micro-sized CeO_2 powder*

Electrochemical deposition of Ni and Ni/CeO_2

Fig. 2 shows the cathodic curves obtained for Ni electro-deposition with and without CeO_2 at two different concentrations. The reduction wave starts at –0.82 V vs. Ag/AgCl when only nickel species are present in the electrolyte. From Fig. 2 we can observe that at the same time with the increase of CeO_2 powder concentration there also takes place a gradual decrease of the cathodic current, and at the same time with the movement towards the more positive potentials of –0.79 and –0.77 V respectively.

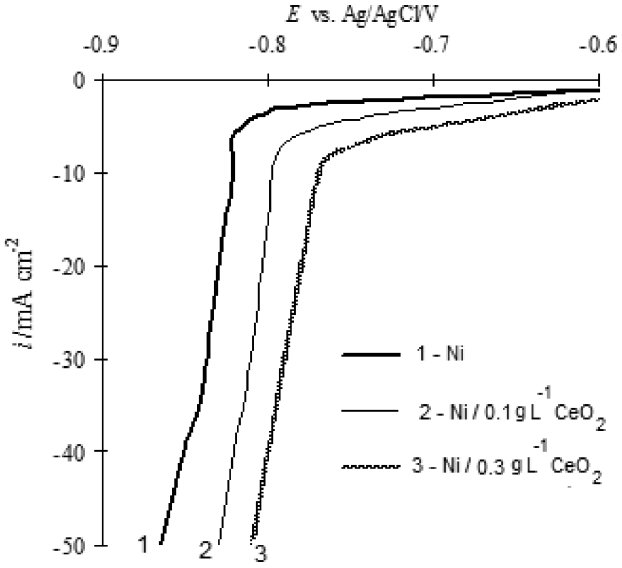

F i g . 2 – *Cathodic curves obtained during nickel deposition onto carbon steel electrode from 150 g L^{-1} $NiSO_4 \cdot 6H_2O$, 30 g L^{-1} H_3BO_3 aqueous solutions, pH = 2; (1) Ni coating; (2) Ni/0.1 g L^{-1} CeO_2 composite coating; (3) Ni/0.3 g L^{-1} CeO_2 composite coating*

Coatings morphology and composition

SEM observation

Fig. 3 shows the morphology of electrodeposited nickel and Ni/0.1 g L^{-1} CeO_2 composite coatings investigated by SEM. The SEM images of carbon steel before electro-deposition (Fig. 3a) Ni and Ni/CeO_2 coatings before corrosion (Fig. 3b, 3c) are presented.

It can be noticed that the addition of ceria particles leads to significant changes in coating morphology.

In case of electro-depositions from solution containing 0.1 g L^{-1} CeO_2 (Fig. 3c) the layer uniformity is more apparent and the feature of a metallic nucleation, forming a matrix in which are embedded certain oxide particle is relatively nuanced.

EDS spectra

The EDS spectra of the Ni coat and Ni/CeO_2 before corrosion in 0.1 mol L^{-1} HCl solution are shown in Fig. 4.

The iron spectrum of a reference sample before corrosion process (uncorroded sample) is presented in Fig. 4a. This spectrum is characteristic of iron from carbon steel.

The EDS spectrum of carbon steel covered with Ni is presented in Fig. 4b. The Ni spectrum is

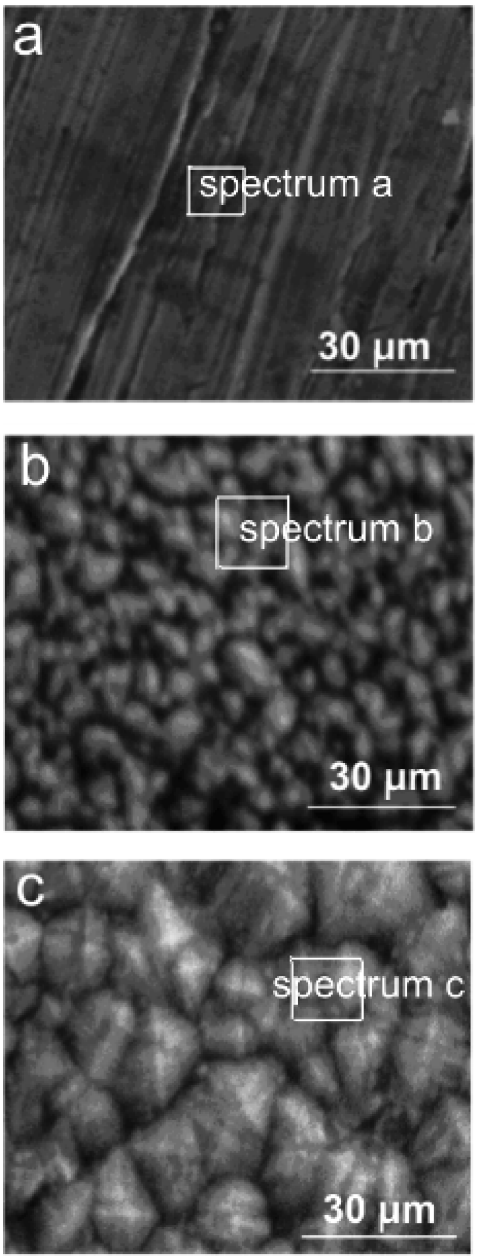

F i g . 3 – *SEM images of: (a) carbon steel substrate; (b) Ni coating; (c) Ni/CeO_2 composite coating deposited from a bath containing 0.1 g L^{-1} CeO_2*

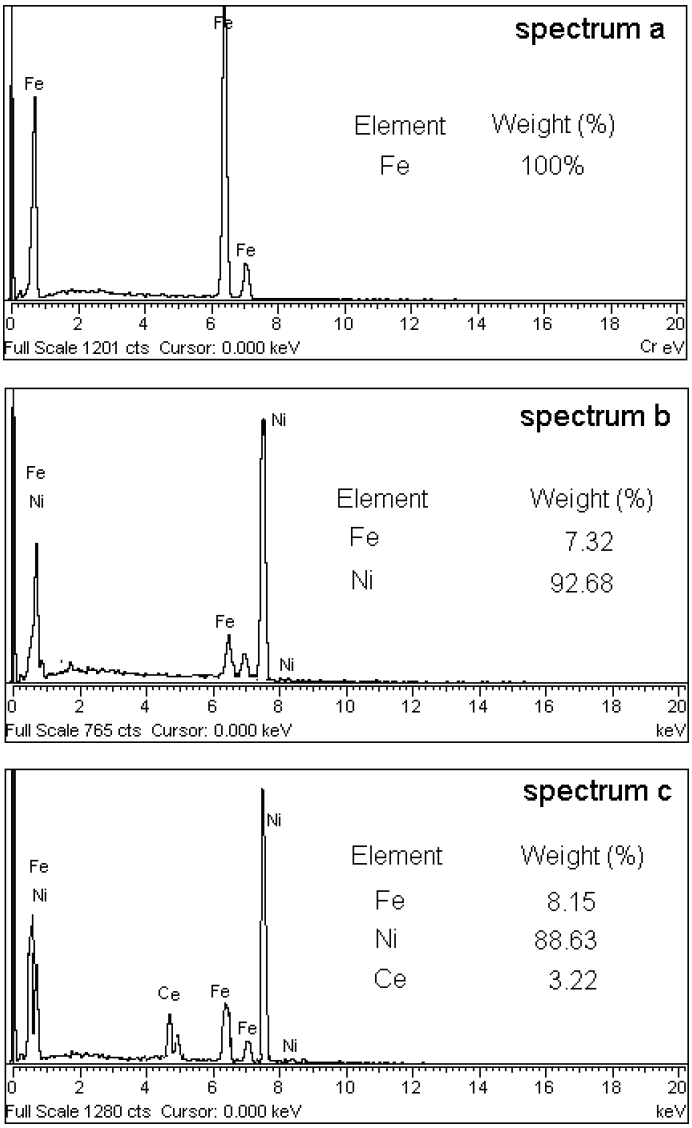

F i g . 4 – *EDS spectra of: (a) carbon steel substrate; (b) Ni coating; (c) Ni/CeO_2 composite coating deposited from a bath containing 0.1 g L^{-1} CeO_2*

also observed in Fig. 4c. Moreover, the EDS spectrum of the composite coating, in Fig. 4c, shows Ce peak, indicating presence of CeO_2 in nickel matrix.

This confirms that the substrate is covered with Ni/CeO_2 composite coating, which is in good agreement with previous considerations.

Corrosion tests

The anticorrosive properties of composite coating in 0.1 mol L^{-1} HCl solution were studied by Tafel polarization and electrochemical impedance spectroscopy.

Tafel polarization

In Tafel domain, the polarisation curves were performed in the potential range –700 mV to –300 mV, with a scan rate of 10 mV s^{-1}. The polarization curves obtained after 1 minute of immersion are presented in Fig. 5.

The performed tests showed that:

Insertion of CeO_2 leads to a corrosion potential shifted to more positive values; the corrosion potential shifted to more positive values correlates, in this case, with a corrosion current decrease; the presence of CeO_2 does not disturb significantly the cathodic reaction but reduces the anodic reaction in a considerable manner; the corrosion current density ($i_{corr.}$) increased with increasing the concentration of CeO_2 (Table 1); the corrosion currents presented in Table 1

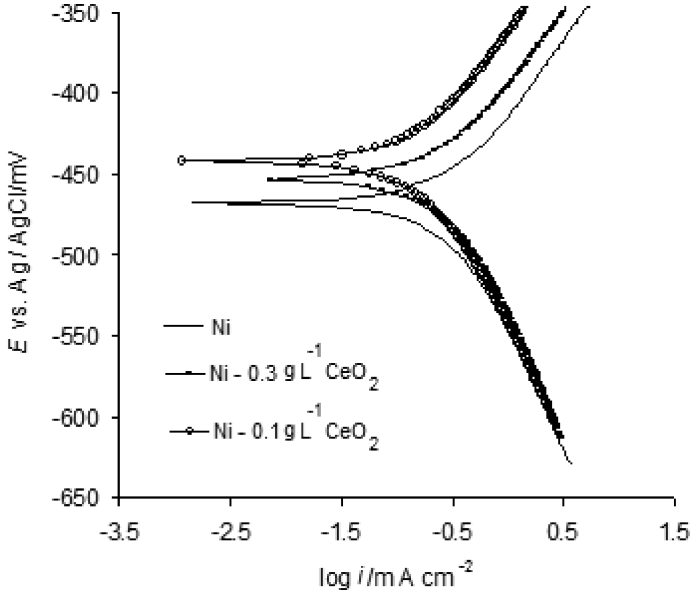

F i g . 5 – *Tafel diagram for Ni coating and Ni/CeO_2 composite coating after corrosion in 0.1 mol L^{-1} HCl solution, at room temperature*

were calculated using VoltaMaster4 software at smoothing 9, calculi zone 120 and segment 80 mV; the percentage protection efficiency (P/%) was calculated using the following relation:

$$P = \frac{i'_{corr} - i_{corr}}{i'_{corr}} \cdot 100 \qquad (1)$$

where i'_{corr} and i_{corr} are the corrosion current densities of the carbon steel surface covered with Ni in the absence and presence of CeO_2, obtained by extrapolation of the anodic and cathodic Tafel lines to the corrosion potential. The percentage protection efficiency (P/%) decreases with increasing the concentration of CeO_2 (Table 1).

T a b l e 1 – *Variation of corrosion current, i_{corr} and protection efficiency, P/% with the concentration of CeO_2 for the carbon steel covered with Ni in absence and presence of oxide, after corrosion in 0.1 mol L^{-1} HCl solution, at room temperature*

Coating	i_{corr}/mA cm^{-2}	P/%
Ni	0.38	0
Ni/0.3 g CeO_2	0.22	42
Ni/0.1 g CeO_2	0.17	55

It can be noticed that the protection efficiency in the presence of 0.1 g CeO_2 exceeds 55 %, which implies a higher corrosion resistance. This can be explained by the appearance at the metal/solution interface of a layer with a different composition from that obtained in the absence of oxide.

Electrochemical impedance measurements

Electrochemical impedance measurements for all investigated samples in 0.1 mol L^{-1} HCl solution were carried out at the open circuit potential, after immersion time of 1 minute, in the frequency range from 10^5 to 10^{-1} Hz, with a value of 10 mV for the amplitude. Fig. 6 shows Nyquist and Bode plots of impedance spectra of investigated coatings in 0.1 mol L^{-1} HCl, at room temperature. It is also apparent from these plots that the Nyquist curves consist of one capacitive loop (one phase angle maximum in Bode format – Fig. 6). More pronounced frequency arcs were obtained for the sample coated with composite layer. Moreover, a shift towards lower frequency of this contribution when oxide was incorporated into Ni matrix can be noticed. This behavior is usually assigned to changes in density and composition of electrode coating.

The impedance parameters derived from EIS measurements R_s, R_p, and C_{dl} and of the protection efficiency were calculated using VoltaMaster 4 software with an error of ±1 %, and are presented in Table 2. (R_s) is the solution resistance of the bulk electrolyte, (C_{dl}) is the double layer capacitance of the electrolyte at the metal surface, and (R_p) is the polarization resistance of the metal.

The protection efficiency (P/%) was determined by the following relationship:

$$P/\% = \left(1 - \frac{R_P^0}{R_P}\right) \cdot 100 \qquad (2)$$

where R_p and R_P^0 represents the polarization resistances in the presence and absence of oxide.

T a b l e 2 – *Electrochemical parameters obtained from impedance measurements for C-steel covered with Ni coat in absence and presence of CeO_2 of different concentrations, at room temperature*

Coating	R_s/Ω cm^2	C_{dl}/μF cm^{-2}	R_p/Ω cm^2	P/%
Ni	1.902	320.1	75.74	0
Ni/0.3 g CeO_2	1.546	269.9	146.36	48.2
Ni/0.1 g CeO_2	1.172	219.9	176.4	57.1

The results show that R_s, C_{dl} decrease and R_p increases with decreasing of CeO_2 concentration, suggesting that the protection efficiency increases. The values of protection efficiency obtained from Tafel polarization and EIS measurements are in good agreement, reaching a maximum value of 57 %, at 0.1 g L^{-1} CeO_2 oxide containing electro-deposition bath.

SEM micrograph of nickel and composite coatings, after corrosion in 0.1 mol L^{-1} HCl solution

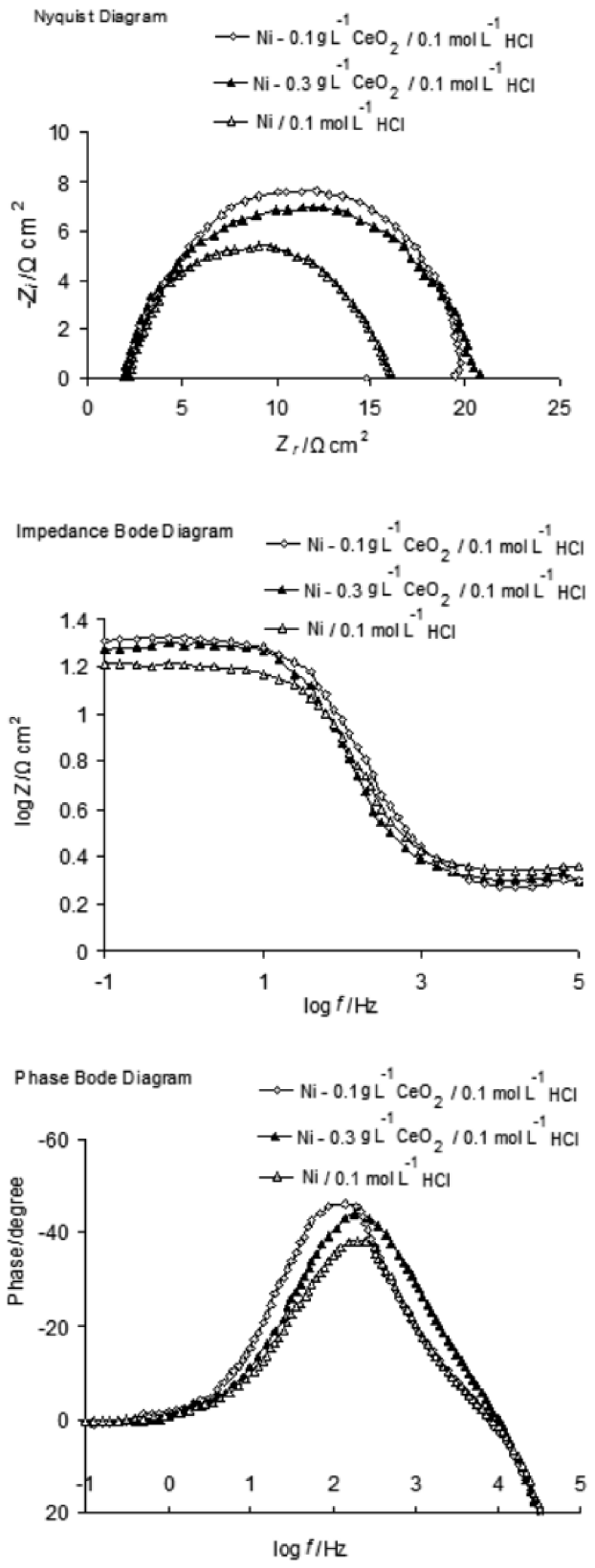

F i g . 6 – *Electrochemical impedance measurements for carbon steel covered with Ni coating in absence and presence of CeO_2 oxide of different concentrations, at room temperature*

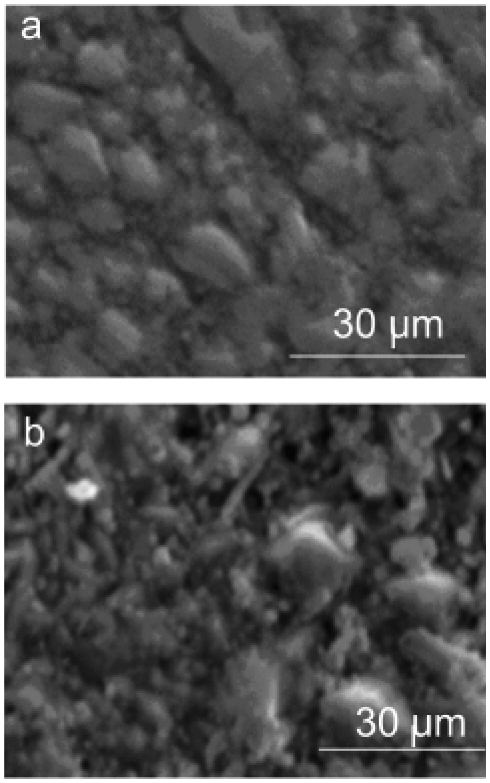

F i g . 7 – *SEM images, after corrosion processes in 0.1 mol L^{-1} HCl solution of: (a) Ni coating; (b) Ni/CeO_2 composite coating deposited from a bath containing 0.1 g L^{-1} CeO_2*

(Fig. 7) revealed the incorporation of solid oxide particles into nickel matrix. The presence of CeO_2 significantly change the texture of Ni coating, resulting in the formation of different layer, in good agreement with SEM images. It can be noticed that the corrosion process in 0.1 mol L^{-1} HCl solution leads to significant changes in coating morphology (see Figs. 3 and 7).

Conclusions

In this work, the corrosion behaviour of Ni coating and Ni/CeO_2 oxide composite coatings was evaluated.

The Tafel curves showed, in this case, that the presence of CeO_2 leads to a shift of corrosion potential towards more positive values, which correlates with a corrosion current decrease with decreasing in CeO_2 concentration.

The corrosion resistance values, obtained from Nyquist plot, confirm an effective protecting power. The gradual presence of the oxide particle on the substrate is characterized in the impedance diagram by a capacitive loop increase, knowing the fact that R_p increases with decreasing of C_{dl}.

The values of protection efficiency obtained from Tafel polarization and EIS measurements are in good agreement, reaching a maximum value of 57 %, at 0.1 g L^{-1} CeO_2 containing electro-deposition bath.

ACKNOWLEDGEMENTS

This work was supported by CNCSIS–UEFISCSU, project number PNII – IDEI 422 code /2008.

List of symbols

EIS – electrochemical impedance spectroscopy
SEM – scanning electron microscopy
EDS – Energy Dispersive X-ray Spectroscopy
i'_{corr} – corrosion current density in the absence of CeO_2, mA cm^{-2}
i_{corr} – corrosion current density in the presence of CeO_2, mA cm^{-2}
P – protection efficiency, %
R_s – solution resistance of the bulk electrolyte, Ω cm^2
R_p^0 – polarization resistances in the absence of CeO_2, Ω cm^2
R_p – polarization resistances in the presence of CeO_2, Ω cm^2
C_{dl} – double layer capacitance, μF cm^{-2}
Z – impedance, Ω cm^2
Z_r – real part of impedance, Ω cm^2
Z_i – imaginary part of impedance, Ω cm^2
f – frequency, Hz

References

1. *Garcia, I., Fransaer, J., Celis, J. P.,* Surf. Coat. Technol. **148** (2001) 171.
2. *Medelien, V.,* Surf. Coat. Technol. **154** (2002) 104.
3. *Zimmerman, A. F., Clark, D. G., Aust, K. T., Erb, U.,* Mat. Lett. **52** (2002) 85.
4. *Hou, K. H., Ger, M. D., Wang, L. M., Ke, S. T.,* Wear **253** (2002) 994.
5. *Socha, R. P., Laajalehto, K., Nowak, P.,* Coll. and Surf. **A 208** (2002) 267.
6. *Vidrine, A. B., Podlaha, E. J.,* J. Appl. Electrochem. **31** (2001) 461.
7. *Zhou, Y., Peng, X., Wang, F.,* Ox. Met. **64** (2005) 169.
8. *Steinbach, J., Ferkel, H.,* Script. Mater. **44** (2001) 1813.
9. *Wang, S. C., Wei, W. C. J.,* Mater. Chem. Phys. **78** (2003) 574.
10. *Zhou, M., Tacconi, N. R., Rajeshwar, K.*, J. Electroanal. Chem. **421** (1997) 111.
11. *Wang, W., Guo, H. T., Gao, J. P., Dong, X. H., Qin, Q. X.,* J. Mater. Sci. **35** (2000) 1495.
12. *Ding, S., Zhang, K., Wang, C.,* J. Wuhan Univ. Tech. Mater. Sci. **22** (2007) 462.
13. *Benea, L.,* J. Appl. Electrochem. **39** (2009) 1671.
14. *Xue, Y. J., Li, J. S., Ma, W., Zhou, Y. W., Duan, M. D.,* J. Mater. Sci. **41** (2006) 1781.
15. *Tu, W. Y., Xu, B. S., Dong, S. Y., Wang, H. D., Bin, J.,* J. Mater. Sci. **43** (2008) 1102.
16. *Lozano-Morales, A., Podlaha, E. J.,* J. Appl. Electrochem. **38** (2008) 1707.
17. *Aruna, S. T., Grips, V. K. W., Selvi, V. E., Rajam, K. S.,* J. Appl. Electrochem. **37** (2007) 991.
18. *Stoyanova, E., Guergova, D., Stoychev, D., Avramova, I., Stefanov, P.,* Electrochim. Acta **55**(5) (2010) 1725.
19. *Stoyanova, E., Nikolova, D., Stoychev, D., Stefanov, P., Marinova, T.,* Corr. Sci. **48**(12) (2006) 4037.
20. *Nikolova, D., Stoyanova, E., Stoychev, D., Stefanov, P., Marinova, T.,* Surf. Coat. Technol. **201** (2006) 1559.
21. *Nickolova, D., Stoyanova, E., Stoychev, D., Avramova, I., Stefanov, P.,* Surf. Coat. Technol. **202** (2008) 1876.
22. *Guergova, D., Stoyanova, E., Stoychev, D., Atanasova, G., Avramova, I., Stefanov, P.,* Bulg. Chem. Comm. **40**(3) (2008) 227.
23. *Hamid, Z. A., Ghayad, I. M.,* Mat. Lett. **53** (2002) 238.
24. *Bercot, P., Pena-Munoz, E., Pagetti, J.,* Surf. Coat. Tech. **157** (2002) 282.
25. *He, L., Liu, H., Chen, D., Chen, Z., Bai, X.,* Surf. Coat. Tech. **160** (2002) 109.
26. *Lee, W. H., Tang, S. C., Chung, K. C.,* Surf. Coat. Tech. **120–121** (1999) 607.
27. *Tseluikin, V. N., Solov`eva, N. D., Gun`kin, I. F.,* Prot. Met. **4** (2007) 388.
28. *Tang, Y. P., Liu, L., Hu, W. B.,* J. Mater. Sci. **40** (2005) 4399.